MECSOL 2022 - Proceedings of the 8th International Symposium on Solid Mechanics
M.L. Bittencourt, J. Labaki, L.C.M. Vieira Jr. and E. Mesquita (Editors), Campinas SP, Brazil, October 17th to 19th, 2022

Viscoelastic Boundary Element Analysis of Three-Dimensional Exponentially Graded Solids

S. A. Santos[1] and C. H. Daros[1]

[1] State University of Campinas - Department of Computational Mechanics, School of Mechanical Engineering - Campinas 13.083-970 SP - Brazil

In the present work, the linear viscoelastic behaviour of three-dimensional isotropic exponentially graded solids under tensile loading conditions is investigated using the boundary element method (BEM). For the exponentially graded solids considered, the elastic modulus varies exponentially along with one, two, or three directions and the Poisson's ratio is assumed to be constant. In order to model the material gradation a fundamental solution for exponentially graded isotropic solids has been readily incorporated into the traditional boundary integral kernels. The viscoelastic behaviour of the material is performed by including in the BEM formulation an approach based on the differential constitutive relations for linear viscoelasticity employing rheological solids models. Numerical examples considering a creep behaviour of the Kelvin-Voigt and Boltzmann material models are presented to demonstrate the accuracy, efficiency and versatility of the used methodology. The results are confirmed by comparisons with the corresponding analytical responses, when possible, or finite element analysis software. Useful information regarding displacement and traction of viscoelastic FGM are obtained here.

Keywords: Viscoelasticity, Boundary element method, Functionally graded viscoelastic materials, Numerical methods, Boundary element analysis

INTRODUCTION

Developments of high technologies applied to material science have provided substantial improvements in advanced materials in the recent decades. Such enhancements stand for enriching the physical, chemical or mechanical properties of a material. Special attention has been given to the enrichment of mechanical properties when related to the gradation of material stiffness. Such features characterize advanced material composites known as functionally graded materials (FGMs).

The concept of FGM was introduced in Japan in 1990 with the development of a composite material applied to an aerospace project. Such composite material was artificially built in order to resist high temperatures in a reduced thickness plate as reported in Miyamoto et al (1999).

Due to the advancement of technologies applied to manufacturing processes we can find distinct compositions of FGMs available today. Some prominent compositions are based on metal–ceramic, metal–metal, ceramic–ceramic, ceramic–polymer, metal–polymer and polymer–polymer structures (Saleh et al., 2020). One of the advantage of FGM is the soft variation of material's stiffness in a determined direction, thus minimizing the effects of interface as presented in the traditional composite materials. Other relevant characteristic is the possibility to combine different classes of materials, thus taking advantage of the intrinsic behaviour of each one. Such combinations of behaviours can be required for many structural components in order to satisfy specific applications. As example we have the combination of brittle and ductile, linear and non linear or elastic and viscoelastic behaviours that are widely used to built components in areas like aerospace, automotive, energy, marine, defence, etc.

The viscoelastic FGMs represent a versatile class of composite materials that have found a wide variety of engineering applications. This kind of material exhibits creep and stress relaxation, thus it experiences strain and stress as a function of time. According to Tschoegl (1989) the fundamental characteristics of viscoelastic material is that they behave as a viscous fluid, elastic solid, or a combination of both when subjected to moderate loading.

In engineering science it is interesting to model and predict the behaviour of viscoelastic FGMs. To make an exact prediction of the stress and strain fields in such materials a complex mathematical analysis is required and it still represents a challenge. In order to overcome this hard task many researchers have applied the traditional finite element method (FEM) or the boundary element method (BEM) to solve problems in distinct areas of engineering.

Most of the works available in the literature related to problems analysis of FGMs solids have been solved by using the FEM. The use of BEM to solve FGM problems has been limited, specially because it requires a fundamental solution

that accurately model the material behaviour. For exponentially graded FGM solids a fundamental solution in three-dimensional domain and in two-dimensional domain are available in Martin et al. (2002) and in Chan et al. (2004), respectively.

Using BEM to evaluate FGMs solids is an advantageous alternative to FEM, especially when analysing the stress field of a problem, which leads to very accurate responses. Moreover, the absence of a domain element mesh can significantly reduce the computational cost.

The objective of the present work is to present an efficient alternative to assess the behaviour of three-dimensional viscoelastic FGM. Thus, the BEM is applied to solve three-dimensional linear elastic and viscoelastic problems for a special FGM which presents the Young modulus exponentially graded in one, two or three directions. Most of the investigations presented in the available literature has been restricted to two-dimensional problems as can be seen in Paulino and Jin (2001), Sladek et al. (2006) and Mahamood and Akinlab (2017). In order to model the continuous material gradation, a special fundamental solution obtained in Martin et al. (2002) and reviewed in Criado et al. (2007a) and Criado et al. (2007b) is implemented in a BEM code. The linear viscoelastic behaviour of the FGM is performed considering the Kelvin–Voigt and Boltzmann rheological material models as used in Neto and Leonel (2019) and Neto and Leonel (2021). The time integration is handled using the time marching process as developed in Mesquita and Coda (2007a) and Mesquita and Coda (2007b).

Useful information regarding displacement and traction fields are assessed herein considering different problems under Heaviside step stress function loading, showing the BEM's excellent numerical performance. The results are compared with analytical responses, when available, and with numerical results extracted from a finite element software to confirm consistency.

BOUNDARY INTEGRAL EQUATIONS FOR VISCOELASTIC FGMS

The viscoelastic FGM considered herein is assumed to be linear and isotropic as presented in Santos and Daros (2022), thus the constitutive equations are based on the linear viscoelasticity for homogeneous materials as described in Christensen (1982) and Tschoegl (1989).

A viscoelastic problem can be described through the following equilibrium equation:

$$\sigma_{ij,j} + b_i = 0, \tag{1}$$

were b_i represents the body force. The elastic and viscous effects are characterized by the kinematic relations for strain (ε_{ij}) and strain rate ($\dot{\varepsilon}_{ij}$), respectively. Here, these relations are described by

$$\varepsilon_{ij} = \frac{1}{2}(u_{i,j} + u_{j,i}), \qquad \dot{\varepsilon}_{ij} = \frac{1}{2}(\dot{u}_{i,j} + \dot{u}_{j,i}). \tag{2}$$

As presented in Aliabadi (2002) to evaluate an elastic problem by the BEM the integral equations for the boundary and internal points of a domain are obtained using the equilibrium equation, Eq.(1), and can be performed applying the weighting residual technique, as follows in Eq.(3):

$$\int_\Omega (\sigma_{ij,j} + b_i) U^*_{ki} d\Omega = 0. \tag{3}$$

In order to perform the integral over the domain Ω in Eq.(3), here is adopted the exponentially graded fundamental solution for FGMs (U^*_{ki}) as a weighting function.

With some manipulation in Eq.(3) and applying the divergence theorem to $(\sigma_{ij}U_{ki})_{,j}$, the Cauchy's relation $\sigma_{ij}n_j = p_i$ and the kinematic relation for strain $\sigma_{ij}U^*_{ki,j} = \sigma_{ij}\varepsilon^*_{kij}$, the integral equation as a function of the stress tensor σ_{ij} can be written as follows:

$$\oint_\Gamma p_i U^*_{ki} d\Gamma - \int_\Omega \sigma_{ij}\varepsilon^*_{kij} d\Omega + \int_\Omega b_i U^*_{ki} d\Omega = 0. \tag{4}$$

According to Mesquita and Coda (2007a), Eq.(4) is the base to introduce the constitutive equations of a viscoelastic rheological model into the boundary integral formulation.

As pointed in Mase and Mase (1999) the response of many viscoelastic materials presents a directly relation with the deviatoric response while the material behaves elastically in dilatation. In order to simplify the solution for practical problems it can be assumed that the material presents the same behaviour in the dilatation as in the deviatoric response. Therefore a constant Poisson's ratio can be applied for viscoelastic analysis, which avoid complex mathematical derivations (Wang and Birgisson, 2007).

The constitutive equations for the rheological models adopted are as follow:

$$\sigma_{ij} = C_{ijkl}\varepsilon_{kl} + \eta_{ijkl}\dot{\varepsilon}_{kl}, \tag{5}$$

for the Kelvin-Voigt model. In Eq.(5) C_{ijkl} and η_{ijkl} are material tensors for the elastic and the viscous properties, respectively, and $\dot{\varepsilon}_{kl}$ is the strain rate. For the Boltzmann model we have

$$\sigma_{ij} = \frac{E_e E_{ve}}{(E_e + E_{ve})}\tilde{C}_{ijkl}\varepsilon_{kl} + \frac{\gamma E_e E_{ve}}{(E_e + E_{ve})}\tilde{C}_{ijkl}\dot{\varepsilon}_{kl} - \frac{\gamma E_{ve}}{(E_e + E_{ve})}\dot{\sigma}_{ij}, \tag{6}$$

where $\tilde{C}_{ijkl} = C_{ijkl}/E_e$ is used to simplify mathematical manipulation and $\dot{\sigma}_{ij}$ is the stress rate. Moreover E_e and E_{ve} correspond to the Young moduli in the elastic and viscoelastic parts of the rheological model, respectively, see Santos and Daros (2022).

In the realm of the BEM, Mesquita and Coda (2007a) observed that it is suitable to impose a proportionality between the viscosity and stiffness parameters to transform the stress rate into a surface force rate on boundary integrals. Thus, the following relation $\eta_{ijkl} = \gamma C_{ijkl}$ has been considered, where γ is the material coefficient viscosity. Through evaluated problems (see Mesquita and Coda (2007b)) it has been verified that such assumption does not affects the accuracy in the convergence of the results.

The coefficient of viscosity is obtained from the creep shear test or the uniaxial tensile test and can vary in time, in such case the proportionality between the viscosity and stiffness no longer exists. Therefore, we have assumed γ constant in the present work, which restricts to viscoelastic materials possessing such characteristics. In addition γ corresponds to the retardation time in a creep test or the relaxation time in a relaxation test (Mase and Mase, 1999).

Incorporating the Eq.(5) into Eq.(4) and considering the symmetry of stress and strain tensors, the kinematical relations, and the symmetry of C_{ijkl} and η_{ijkl}, we can write the boundary integral equation for the viscoelastic Kelvin-Voigt model as follows:

$$C_{ki}u_i(\boldsymbol{x}') + \gamma C_{ki}\dot{u}_i(\boldsymbol{x}') = \oint_\Gamma p_i U^*_{ki} d\Gamma - \oint_\Gamma u_i P^*_{ki} d\Gamma - \gamma \oint_\Gamma \dot{u}_i P^*_{ki} d\Gamma. \tag{7}$$

Following the above procedure, it is necessary to insert Eq.(6) into Eq.(4) to obtain the boundary integral equation for the viscoelastic Boltzmann model. Here we have to take into account the kinematical relations and use the following symmetry concepts $\varepsilon^*_{kij}E_e\tilde{C}_{ijlm}\varepsilon_{lm} = \sigma^*_{kij}u_{i,j}$, $\gamma\varepsilon^*_{kij}E_e\tilde{C}_{ijlm}\dot{\varepsilon}_{lm} = \gamma\sigma^*_{kij}\dot{u}_{i,j}$ and $\varepsilon^*_{kij}\dot{\sigma}_{ij} = U^*_{ki,j}\dot{\sigma}_{ij}$. Thus, it yields

$$C_{ki}u_i(\boldsymbol{x}') + \gamma C_{ki}\dot{u}_i(\boldsymbol{x}') = \frac{E_e + E_{ve}}{E_{ve}} \oint_\Gamma U^*_{ki} p_i d\Gamma - \oint_\Gamma P^*_{ki} u_i d\Gamma - \gamma \oint_\Gamma P^*_{ki}\dot{u}_i d\Gamma + \gamma \oint_\Gamma U^*_{ki}\dot{p}_i d\Gamma. \tag{8}$$

In Eq.(7) and Eq.(8) $\boldsymbol{x}'$ is the source point in a domain or over the boundary and C_{ki} is the coefficient tensor of the free term which depends on the boundary smoothness.

The kernels of the fundamental solutions inserted in Eq.(7) and Eq.(8) reproduce the behaviour of a specific class of isotropic FGM which considers a constant Poisson's ratio (ν) and the Lamé moduli varying exponentially in a continuous function, such that

$$\mu(x) = \mu_0 e^{(2\beta \cdot x)} \qquad \text{and} \qquad \lambda(x) = \lambda_0 e^{(2\beta \cdot x)}, \tag{9}$$

where the vector β represents the material gradient coefficients $(\beta_1, \beta_2, \beta_3)$, with 1, 2 and 3 corresponding the three Cartesian directions. The assumption Eq.(9) is typical in the engineering literature devoted to FGM (Martin et al, 2002). Moreover, according to Chan et al (2004), a constant Poisson's ratio is reasonable and it is widely used in the literature dedicated to this class of material.

The kernels U^*_{ki} and P^*_{ki} are the displacement and traction fundamental solution tensors, respectively. According to Martin et al. (2002) the displacement kernel is defined as follows:

$$U^*_{ki}(x,x') = e^{\left[-\beta \cdot (x+x')\right]} \left[U^0_{ki}(x,x') + U^g_{ki}(x,x')\right], \tag{10}$$

where k is the displacement component at point x due to a unit point force acting in the i-direction at point x'. Moreover, $U^0_{ki}(x,x')$ is the displacement fundamental solution for a homogeneous medium (Aliabadi, 2002) and is written as follows

$$U^0_{ki}(\boldsymbol{x},\boldsymbol{x}') = \frac{1}{16\pi\mu_0(1-\nu)r}\left[(3-4\nu)\delta_{ki} + r_{,k}r_{,i}\right]. \tag{11}$$

The term $U^g_{ki}(x,x')$ corresponds to the grading component and is expressed as follows

$$U^g_{ki}(x-x') = -\frac{1}{4\pi\mu_0 r}(1-e^{-\beta r})\delta_{ki} + A_{ki}(x-x'), \tag{12}$$

where $A_{ki}(x-x')$ is a sum of five single and double integrals, including first kind Bessel and hyperbolic functions as described in Criado (2007a) and Criado (2007b). When $\beta = 0$ Eq. (12) vanishes, which restores to the solution for homogeneous medium in Eq.(10).

It is observed that Eq.(11) and Eq.(12) have the same weak singularity at $r = 0$.

Following the displacement kernel, the traction kernel is also split into two components, such that

$$P^*_{ki} = e^{\beta\cdot(x-x')}\left[P^0_{ki}(x,x') + P^g_{ki}(x,x')\right], \tag{13}$$

where $P^0_{ki}(x,x')$ represents the homogeneous part and according to Aliabadi (2002) is written in the following way

$$P^0_{ki}(\boldsymbol{x},\boldsymbol{x'}) = \frac{-1}{8\pi(1-\nu)r^2}\left\{\frac{\partial r}{\partial n}\left[(1-2\nu)\delta_{ki} + 3r_{,k}r_{,i}\right] - (1-2\nu)(n_i r_{,k} - n_k r_{,i})\right\}. \tag{14}$$

The grading term $P^g_{ki}(x,x')$ is given by Martin et al. (2002)

$$P^g_{ki} = \mu_0\left[\frac{\partial U^g_{ki}}{\partial x_l} + \frac{\partial U^g_{li}}{\partial x_k} - \beta_k(U^0_{li} + U^g_{li}) - \beta_l(U^0_{ki} + U^g_{ki})\right] n_l(x) + \lambda_0\left[\frac{\partial U^g_{ji}}{\partial x_j} - \beta_j(U^0_{ji} + U^g_{ji})\right]\delta_{kl} n_l(x), \tag{15}$$

with $n_l(x)$ being the unit outward normal vector.

The homogeneous component of the traction kernels Eq.(14) presents a strong singularity while the graded component Eq.(15) is weakly singular.

To perform the numerical integration procedure over Eq.(7) and Eq.(8), the boundary is divided into triangular or quadrilateral quadratics elements. Moreover, in this work we have used continuous and discontinuous elements. The standard procedure to separate the numerical integration into regular and singular has been considered here. In order to evaluate the regular numerical integration over an element the Gaussian quadrature has been used as follows:

$$\int_\eta\int_\xi U^*_{ki}\phi_k|J|d\xi d\eta \approx \sum_{\alpha=1}^{n}\sum_{\rho=1}^{n} U^*_{ki}\phi_k|J|w_\rho w_\alpha, \qquad \int_\eta\int_\xi P^*_{ki}\phi_k|J|d\xi d\eta \approx \sum_{\alpha=1}^{n}\sum_{\rho=1}^{n} P^*_{ki}\phi_k|J|w_\rho w_\alpha \tag{16}$$

where $-1 \le \xi \le 1$ and $-1 \le \eta \le 1$ are the homogeneous coordinates, J is the Jacobian of the transformation from Cartesian coordinates to homogeneous coordinates, w is the Gauss weight, n is the number of Gauss points ($n = 6$ for quadrilateral elements and $n = 4$ for triangular elements in this work) and ϕ is the interpolation function for each functional node k. The interpolation functions for the geometrical and functional nodes for quadrilateral continuous elements, as presented in Aliabadi (2002), are written in Eq.(17).

$$\begin{aligned}
&\phi_1 = \frac{1}{4}\xi(\xi-1)\eta(\eta-1), \quad \phi_2 = \frac{1}{2}(1-\xi^2)\eta(\eta-1), \quad \phi_3 = \frac{1}{4}\xi(\xi+1)\eta(\eta-1),\\
&\phi_4 = \frac{1}{2}\xi(\xi+1)(1-\eta^2), \quad \phi_5 = \frac{1}{4}\xi(\xi+1)\eta(\eta+1), \quad \phi_6 = \frac{1}{2}(1-\xi^2)\eta(\eta+1),\\
&\phi_7 = \frac{1}{4}\xi(\xi-1)\eta(\eta+1), \quad \phi_8 = \frac{1}{2}\xi(\xi-1)(1-\eta^2), \quad \phi_9 = (1-\xi^2)\eta(1-\eta^2).
\end{aligned} \tag{17}$$

When using quadrilateral discontinuous elements the interpolation functions for functional nodes have been obtained using $\xi = (3/2)\xi$ and $\eta = (3/2)\eta$ in Eq.(17). In the other hand the interpolation functions of functional nodes used for triangular discontinuous elements are as follows:

$$\begin{aligned}
&\phi_1 = \frac{8}{5}\left(\xi-\frac{1}{8}\right)\left[\frac{16}{5}\left(\xi-\frac{1}{8}\right)-1\right], \qquad \phi_2 = \frac{8}{5}\left(\eta-\frac{1}{8}\right)\left[\frac{16}{5}\left(\eta-\frac{1}{8}\right)-1\right],\\
&\phi_3 = \left[\frac{7}{5}-\frac{8}{5}\left(\xi+\eta\right)\right]\left[\frac{9}{5}-\frac{16}{5}\left(\xi+\eta\right)\right], \qquad \phi_4 = \frac{256}{5}\left(\xi-\frac{1}{8}\right)\left(\eta-\frac{1}{8}\right),\\
&\phi_5 = \frac{32}{5}\left(\eta-\frac{1}{8}\right)\left[\frac{7}{5}-\frac{8}{5}\left(\xi+\eta\right)\right], \qquad \phi_6 = \frac{32}{5}\left(\xi-\frac{1}{8}\right)\left[\frac{7}{5}-\frac{8}{5}\left(\xi+\eta\right)\right].
\end{aligned} \tag{18}$$

The weakly singular integrals involving the kernel U^*_{ki} are dealt with a triangle to square transformation as described in Aliabadi (2002), in which the singularity is cancelled out by the Jacobian of the transformation. In addition, the rigid body motion procedure is applied to evaluate the sum of the coefficient tensor of the free term C_{ki} and the Cauchy principal value integral present in the kernel P^*_{ki} when $r \to 0$.

The here adopted technique is based on the traditional triangle to square transformation for continuous element as presented in Aliabadi (2002) and has been adapted for discontinuous element. Figure (1) illustrates the element subdivision procedure for discontinuous elements.

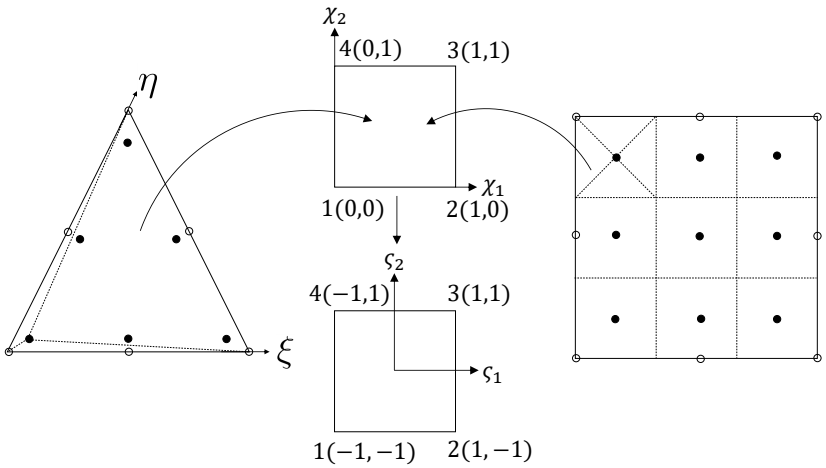

Figure 1: Element subdivision for singular integration.

The quadrilateral element is divided into 9 identical squares, then the squares that contain the functional nodes are divided into 4 triangles such that the functional node is located in one of triangle vertex. Each triangle is transformed into a square in (χ_1,χ_2) coordinate system, such that the Jacobian of the transformation (ξ,η) to (χ_1,χ_2) becomes zero in the collocation point. Moreover, in order to use the Gaussian quadrature again a new transformation to the coordinates $(\varsigma_1,\varsigma_2)$ has been applied. While the integration is performed over the triangles another integration procedure using simple Gaussian quadrature is performed over the empty squares (squares that not contain the collocation point). The numerical integration using the subdivision of an element has been implemented as follows:

$$\int_\eta\int_\xi U^*_{ki}\phi_k|J|d\xi d\eta \approx \sum_{triangle=1}^{4}\sum_{\alpha=1}^{n}\sum_{\rho=1}^{n} U^*_{ki}\phi_k|J|(\varsigma_1+1)\frac{A}{4}w_\rho w_\alpha \quad + \sum_{square=1}^{8}\sum_{\alpha_s=1}^{n_s}\sum_{\rho_s=1}^{n_s} U^*_{ki}\phi_k|J||J_s|w_{\rho_s}w_{\alpha_s}, \tag{19}$$

where A is the area of the triangle in dimensionless coordinates (ξ,η), J_s is the Jacobian of the transformation from (ξ,η) to (ξ',η') in the empty squares, n_s and w_{p_s} are the Gauss points and Gauss weight, respectively. In the present work we have used $n_s = 4$ integration points for each square. The strong singularity present in the traction kernel P^*_{ki} has been treated via rigid body motion procedure.

The grading term U^g_{ki} has been completely integrated using simple Gaussian quadrature. Due to a singular integral of the type $1/\sqrt{\delta}$ present in the term P^g_{ki} (see Criado (2007a) page 155, eq. 36) we have applied the special Gauss-Jacobi quadrature to treat the singularity. For both quadratures (i.e. Gauss and Gauss-Jacobi) we have used 10 points to integrate the terms in U^g_{ki} and P^g_{ki}.

After the integration over each element, Eq.(7) and Eq.(8) are conveniently written in a matrix form such that we have for the Kelvin-Voigt rheological model the following

$$[H]\{u(t)\} + \gamma[H]\{\dot{u}(t)\} = [G]\{p(t)\}, \tag{20}$$

and for the Boltzmann rheological model

$$[H]\{u(t)\} = \frac{E_e + E_{ve}}{E_{ve}}[G]\{p(t)\} - \gamma[H]\{\dot{u}(t)\} + \gamma[G]\{\dot{p}(t)\}. \tag{21}$$

Using the time marching process with $\dot{u}_{s+1} = (u_{s+1} - u_s)/\Delta t$ and $\dot{p}_{s+1} = (p_{s+1} - p_s)/\Delta t$, where $s+1$ represents the current instant and Δt is the time increment, Eq.(20) and Eq.(21) are reduced to

$$[A]\{x\}_{s+1} = \{\bar{F}\}_{s+1} + \{F\}_s, \tag{22}$$

where $\{F\}_s = \gamma/\Delta t[H]\{u\}_s$ and $\{F\}_s = \gamma/\Delta t[H]\{u\}_s - \gamma/\Delta t[G]\{p\}_s$ are used in the Kelvin-Voigt and Boltzmann formulation, respectively.

NUMERICAL RESULTS

In order to verify the versatility of the formulation shown before, in this section three practical problems in elasticity and viscoelasticity fields are investigated.

Regular hexahedron subjected to a constant traction

The first problem corresponds to a regular hexahedron subjected to a constant traction on the upper face while the displacements on the lower face are restricted. In this case study the objective is to analyse the behaviour of an elastic FGM where the gradation is adopted to vary in one direction (z) or over the three directions (x, y, z). The hexahedron has side $L = 1$ [cm] and is subjected to traction $P = 100$[Pa]. The considered shear modulus in the origin of the coordinate system is $\mu_0 = 1$ [MPa] and in the upper face is imposed $\mu(z) = 25.53\mu_0$. At first, in order to compare with the displacement analytical solution, where $U(z) = P/(4\mu_0\beta_z)(1-e^{-2\beta_z z})$, the Poisson's ratio assumed is $\nu = 0$. The displacement response and the numerical error can be seen in Fig. 2a and Fig. 2b, respectively.

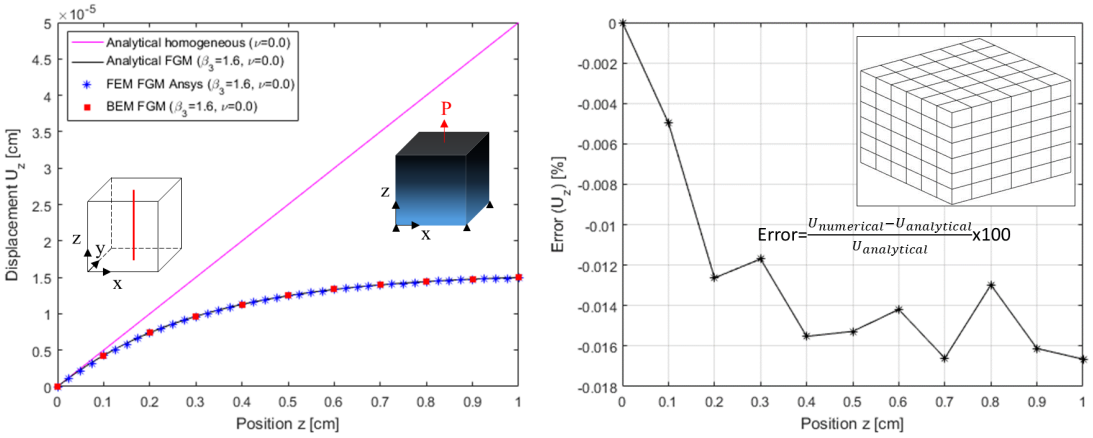

(a) U_z (b) Numerical error

Figure 2: Displacement in unidimensional analysis.

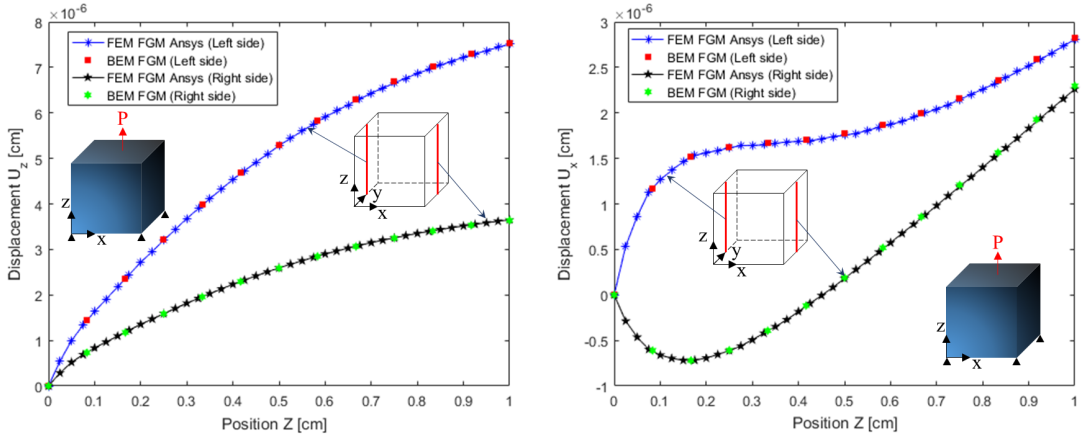

(a) U_z. (b) U_x.

Figure 3: Displacement in three-dimensional analysis.

Another consideration is related to the material gradation in the three directions where $\mu(x) = 2.22\mu_0$, $\mu(y) = 4.05\mu_0$ and $\mu(z) = 7.39\mu_0$. Here the Poisson's ratio assumed is $\nu = 0.3$. For this case there is no analytical solution, thus the BEM responses of displacements are compared with finite element software results as shown in Fig. 3.

Through Fig. 3a and Fig. 3b one can notice the effects of material gradation on the displacements. Although symmetric boundary conditions have been applied, the displacement behaviours in the two regions in opposite sides present significant effects of the material gradation.

It can be verified on Fig. 2 and Fig. 3 the displacements are to the order of 10^{-5}[cm] resulting in deformations lower than 10^{-5} [cm/cm], which is small enough to be considered a linear problem.

In this problem only quadrilateral quadratic continuous elements have been applied. The mesh used is composed with 216 boundary elements as illustrated in Fig. 2b.

Disc subjected to a uniform displacement

In the second case study the objective is to verify the behaviour of a disc graded in the radial direction under a constant displacement ($u_z = -8.488x10^{-2}$[mm]) applied on the upper face. In this case the material is assumed linear elastic with $\mu_0 = 22.2222$ [MPa] at the centre and $\mu_r = 40\mu_0$ at the extremity $r = 20$[mm]. The Poisson's ratio assumed is $\nu = 0.35$. Since the fundamental solution has been derived in Cartesian coordinate system, in this problem the radial gradation of the material is approximately assessed using the subregion methodology as presented in Santos (2021). For this problem there are analytical solutions for the normal displacement ($u(z) = u_z z/h$), radial displacement ($u(r) = -\nu u_z r/h$) and traction on the lower surface ($\sigma_z(r) = u_z\mu_0(1+\nu)e^{2\beta_r r}/h$), where $\beta_r = 1/(2r)ln(\mu_r/\mu_0)$. The mesh used in this problem is composed of 1240 quadrilateral and 80 triangular quadratic discontinuous elements distributed in 40 subregions, as shown in Fig. 4a. Figure 4b shows the traction response as function of the radius distance as well as the numerical error.

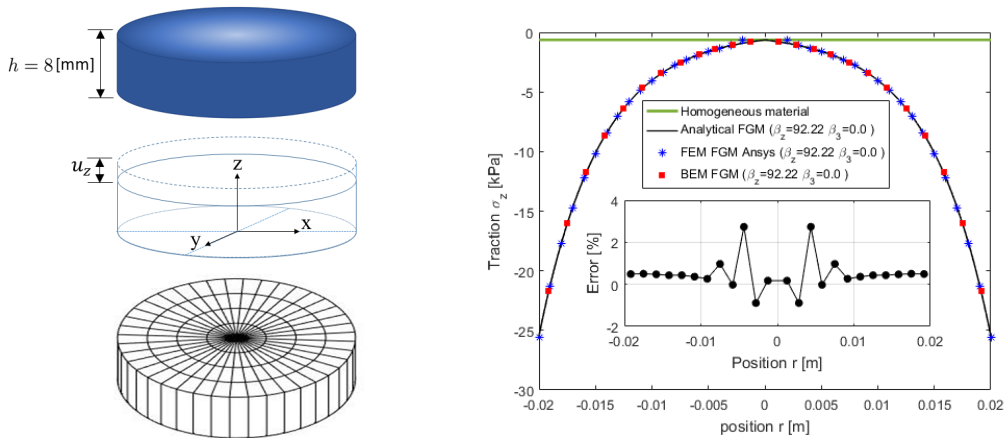

(a) Geometry and mesh.

(b) Traction

Figure 4: Disc geometry with boundary conditions and traction results.

Normal and radial displacements are illustrated in Fig. 5a and Fig. 5b, respectively. In this case study the material gradation has drastically distorted the traction behaviour as seen in Fig. 4b.

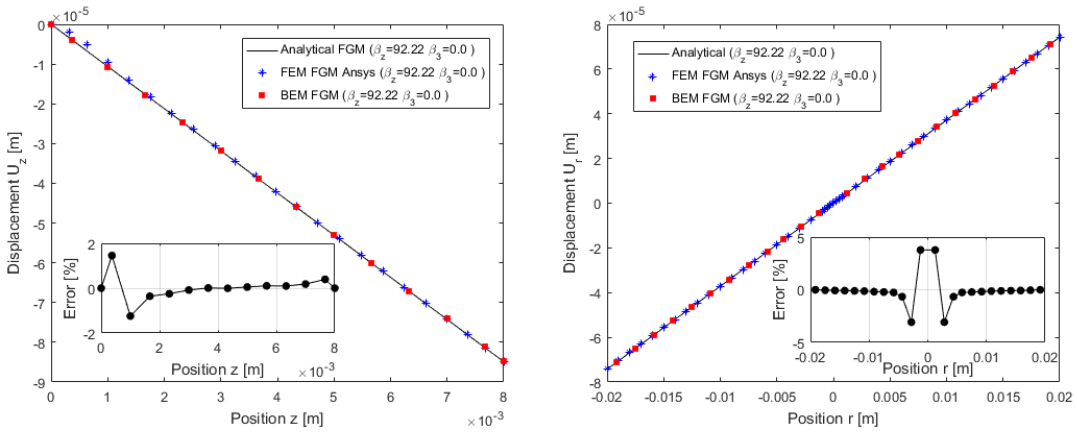

(a) Normal displacement on line (0,0,z).

(b) Radial displacement in r on the upper surface.

Figure 5: Displacement.

Hollow cylinder subjected to a uniform internal pressure

The objective of this problem is to demonstrate the consistence of the BEM formulation incorporated with the previously described rheological models to numerically reproduce the viscoelastic behaviour of FGM. The problem consists of a hollow cylinder undergoing creep deformation subjected to a uniform internal pressure $PH(t) = 100$[kPa], where $H(t)$ is the Heaviside function. Using symmetric boundary conditions only a quarter of the cylinder has been modelled. The internal and external radius are $r_i = 5$ [mm] and $r_e = 20$ [mm], respectively. The height is $h = 8$[mm]. Figure 6a illustrates the geometry and boundary conditions assumed. The boundary mesh is composed of 220 quadrilateral quadratic discontinuous elements distributed in 10 subregions as can seen in Fig. 6b. In order to verify the viscoelastic behaviour, the materials properties assumed in this problem are $\nu = 0.35$, $\gamma = 10$[s], $\Delta t = 1$[s] and $E_0^{vis} = 60$[kPa], $E_0^{el} = 250$[kPa]. E_0^{el} corresponds to the stiffness only in Boltzmann model and E_0^{vis} corresponds to the stiffness in both models. The cylinder is graded in radial direction such that the stiffness in r_e is 15.894 times the stiffness in r_i. Figure 7 illustrates the displacements in internal and external walls monitored during $T = 100$[s].

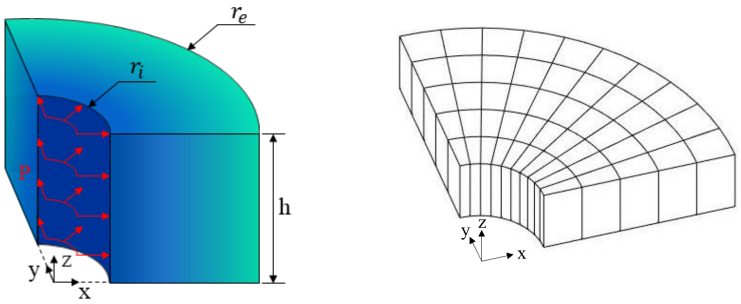

(a) Geometry of the problem.

(b) Boundary element mesh

Figure 6: Problem considered with mesh and boundary conditions.

This problem has analytical solutions for the radial displacement as well as the Hoop stress as described in Santos (2021). It is noted in the Boltzmann model response the elastic reaction represented by an instantaneous displacement. The numerical Hoop stress results for both rheological models extracted from the nodes on the middle of the symmetry surface ($y = 0$) are shown in Fig. 8. The equivalence in stress for both material models exhibited in Fig. 8 are in accordance since the Boltzmann model is composed of a Kelvin-voigt model connected to an elastic element. For Boltzmann model the stress in the viscoelastic and elastic components is the same.

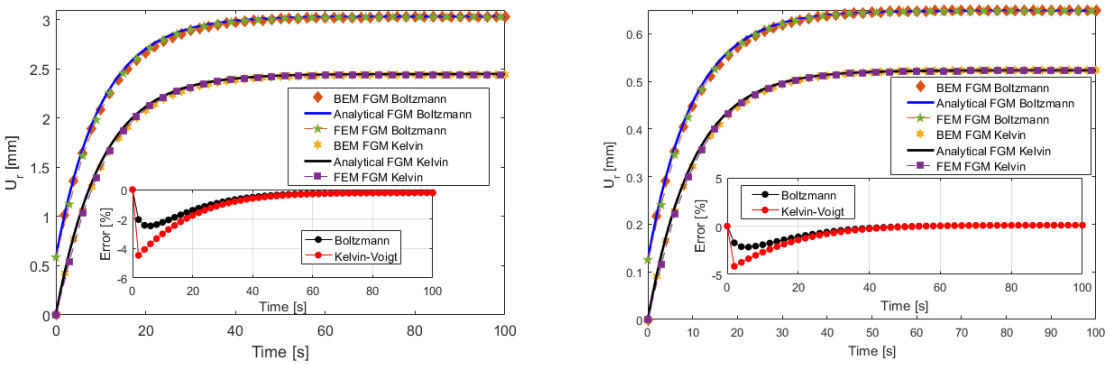

(a) Internal wall.

(b) External wall

Figure 7: Viscoelastic displacements.

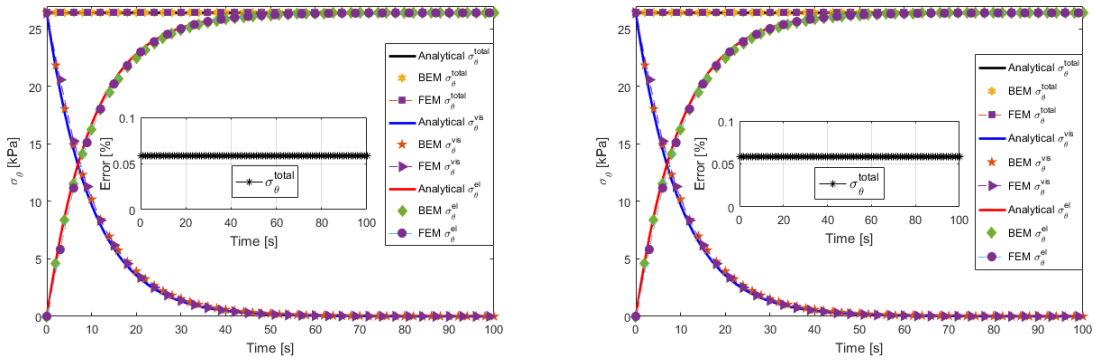

(a) Kelvin rheological model

(b) Boltzmann rheological model

Figure 8: Viscoelastic Hoop stress.

CONCLUSIONS AND DISCUSSIONS

In the present work a three-dimensional viscoelastic boundary element analysis of exponentially FGMs has been demonstrated. The formulation used to reproduce the time dependence of the material is based on the rheological models and a time marching process. The FGM properties has been included into the formulation using a special fundamental solution. In order to solve practical problems the BEM formulation has been implemented in a Matlab code. To avoid the high computational cost required in the fundamental solution processing a parallel multiprocessing based on the Single Program Multiple Data function has been incorporated into the BEM code.

Practical elastic and viscoelastic problem responses have shown the consistence and versatility of the formulation in comparison with analytical and finite element software package results.

As can be observed the effects of material gradation presents substantial influence on the displacement and specially on the traction field results. In the disc problem subjected to a uniform displacement the responses have shown the proportionality between the traction field and material gradation. For this case the traction results along the radius direction are up to 40 times greater than the results for homogeneous material.

It is important to notice that the viscosity component of the materials is assumed to be constant, thus it is not affected by the material gradation although it can be dependent on temperature.

In this work we have assessed the traction in the boundary and even using symmetry conditions the results agree very well with the analytical one, nonetheless it is interesting to assess the stress field in the domain. It is expected in future work to implement a complete formulation including the stress kernels in order to investigate the influence of material gradation on the stress field in FGM solids, which is one of the recognizable qualities of the BEM.

ACKNOWLEDGMENTS

This work was supported by São Paulo Research Foundation (FAPESP) grant No. 2016/23745-0. In addition, this study was financed in part by the Coordenação de Aperfeiçoamento de Pessoal de Nível Superior – Brasil (CAPES) – Finance Code 001.

REFERENCES

Aliabadi, M. H., 2002, "The Boundary Element Method: Applications in Solids and Structures", Ed. John Wiley and Sons, New Jersey, USA.

Chan, Y. S. and Gray, L. J. and Kaplan, T. and Paulino, G. H., 2004, "Green's function for a two-dimensional exponentially graded elastic medium", Proc. Royal Soc. Lond. A., Vol. 460, pp. 1689-1706.

Christensen, R. M., 1982, "Theory of Viscoelasticity", Ed. Academic Press, New York, USA.

Criado, R. and Mantic, V. and Gray, L. J. and París, F., 2007a, "Green's Function Evaluation for Three Dimensional Exponentially Graded Elasticity", Int. J. Numer. Meth. Engng., Vol. 74, pp. 1560-1591.

Criado, R and Ortiz, J E and Mantic, V and Gray, L J and París, F, 2007b, "Boundary element analysis of three-dimensional exponentially graded isotropic elastic solids", Comput. Model. Eng. Sci., Vol. 22, pp. 151-164.

Mahamood, R. M. and Akinlab, E. T., 2017, "Functionally Graded Materials", Ed. Springer International Publishing, Switzerland.

Mase, G. T. and Mase, G. E., 1999, "Continuum Mechanics for Engineers", Ed. CRC Press, Boca Raton, USA.

Martin, P. A. and Richardson, J. D. and Gray, L. J. and Berger, J., 2002, "On Green's Function for a three-dimensional exponentially graded elastic solid", Proc. Royal Soc. Lond. A., Vol. 458, pp. 1931-1947.

Mesquita, A. D. and Coda, H.B., 2007a, "A boundary element methodology for viscoelastic analysis: Part I with cells", Appl. Math. Modell., Vol. 31, pp. 1149-1170.

Mesquita, A. D. and Coda, H.B., 2007b, "A boundary element methodology for viscoelastic analysis: Part II without cells", Appl. Math. Modell., Vol. 31, pp. 1171-1185.

Miyamoto, Y. and Kaysser, W.A. and Rabin, B.H, 1999, "Functionally Graded Materials: Design, Processing and Applications", Ed. Kluwer Academic Press, Boston, USA.

Neto, A. R. and Leonel, E. D., 2019, "The mechanical modelling of nonhomogeneous reinforced structural systems by a coupled BEM formulation", Engng. Anal. Bound. Elem., Vol. 109, pp. 1-18.

Neto, A. R. and Leonel, E. D., 2021, "Three dimensional nonlinear BEM formulations for the mechanical analysis of nonhomogeneous reinforced structural systems", Engng. Anal. Bound. Elem., Vol. 123, pp. 200-219.

Paulino, G. H. and Jin, Z. H., 2001, "Correspondence principle in viscoelastic functionally graded materials", ASME J. Appl. Mech., Vol. 68, pp. 129-132.

Saleh, B. and Jiang, J. and Fathi, R. and Al-Hababi, T. and Xu, Q. and Wang, L. and Song, D. and Ma, A., 2020, "30 Years of functionally graded materials: An overview of manufacturing methods, Applications and Future Challenges", Composites Part. B: Engineering, Vol. 201, pp. 108376.

Santos, S. A., 2021, "Método dos Elementos de Contorno Aplicado à Viscoelasticidade Quase-estática Tridimensional em Materiais Gradualmente Funcionais" (Ph.D. thesis), Campinas, SP, Brazil: School of Mechanical Engineering, State University of Campinas; 2021.

Santos, S. A. and Daros, C. H., 2022, "Boundary element method applied to three-dimensional crack analysis in exponentially graded viscoelastic materials", Engng. Fract. Mech., Vol. 263, pp. 108284.

Sladek, J. and Sladek, V. and Zhang, C. and Schanz, M., 2006, "Meshless local Petrov-Galerkin method for continuously nonhomogeneous linear viscoelastic solids", Comput. Mech., Vol. 37, pp. 279-289.

Tschoegl, N. W., 1989, "The phenomenological theory of linear viscoelastic behaviour: An introduction", Ed. Springer-Verlag, Berlin, Germany.

Wang, J. and Birgisson, B., 2007, "A time domain boundary element method for modeling the quasi-static viscoelastic behavior of asphalt pavementss", Eng. Anal. Bound. Elem., Vol. 31, pp. 226–40.

RESPONSIBILITY NOTICE

The authors are the only parties responsible for the printed material included in this paper.

RESPONSE TO REVIEWERS

Following the manuscript, we have included a response to reviewers in which we address the comments the reviewers made. In our response to reviewers, the reviewers's comments are in black and our responses follow below, in blue, and are prefaced by "Author response.".

Comment from Reviewer 1

The article present a viscoelastic linear analysis for 3D exponentially graded solids. The BEM is used to this end. The article is well written and brings interesting results. Consider, for future publications, that the axes xyz are not well defined on Figure 4 and Figure 6.

Author response: The coordinate system has been updated and adequately defined on Figure 4 and Figure 6.

Comments from Reviewer 2

The manuscript presents a study about exponentially graded isotropic solids with viscoelastic behavior (creep analyses considered Kelvin-Voigt and Boltzmann models) modeled by Boundary Element Method. The Kelvin fundamental solution is considered to model 3D solids. The manuscript is interesting in academic terms. The Biot strain mesure presented in Eq. (2) is suitable for small strains, but depending on material characteristics and creep deformation it would not suitable for moderate strains (40%). For instance, example 1 considers an hexahedron with side equal to 1cm and presents displacements over 1cm. Certainly, Biot strain measure and its conjugate stress pair (Jaumann) are not suitable for this level of high strains.

Author response: In the example 1 we have found displacements to the order of 10^{-5} [cm] and consequently the deformations are lower than $5x10^{-5}$, which justify the solution of linear problems as described in the 4th paragraph of example 1.

Other problematic point is the consideration of constant Poisson ratio for any point of the domain, especially when material vary its density along a single direction.

Author response: According to Martin et al (2002) and Chan et al (2004) the use of a constant Poisson's ratio for FGM is reasonable and it is widely adopted in the literature about this class of material. This argument has been written on page 3 paragraph 4.

First two numerical examples deal with uniaxial tractions. A severe problem of BEM is related to shear state. For future works, authors are claimed to present responses related to shear state problem.

Author response: The present work has the objective to demonstrate the basic behaviours of elastic and viscoelastic 3D FGMs graded in one or more directions. For this end the examples presented are suitable, moreover it is expected in future work to expand the study presenting solutions related to shear state problem.

In Fig. 7 would be interesting to present graphs with for the same displacement interval.

Author response: The results on Figure 7 have been reorganised, such that the displacement on internal and external walls are illustrated in separated form in order to fulfil the same displacement interval.

We appreciate the comments and suggestions from the reviewers. We hope the responses are in accordance with the reviewers requests.

We are thankful to the reviewers for taking your time to review our manuscript and for the valuable comments and suggestions provided.